Beyond Qubits: Building Quantum Refrigerators in Higher Dimensions

Tanoy Kanti Konar[1], Srijon Ghosh[1], Amit Kumar Pal[2], Aditi Sen(De)[1]

[1]*Harish-Chandra Research Institute, HBNI, Chhatnag Road, Jhunsi, Allahabad 211 019, India and*
[2] *Department of Physics, Indian Institute of Technology Palakkad, Palakkad 678 557, India*

We design quantum refrigerators based on spin-j quantum XYZ and bilinear-biquadratic models with individual spins attached to bosonic thermal baths. By considering both local and global master equations, we illustrate an enhancement in the performance of the refrigerators with an increase in the spin dimension irrespective of the choice of the spin models. To assess the performance of the refrigerators, we introduce a distance-based measure to quantify the local temperature of a particle with arbitrary spin quantum number j. Interestingly, we find that the local temperature quantifier, defined via minimizing the distance between a spin-j thermal state and the evolved state of the spin-j particle in the steady state, coincides with the population-based definition of local temperature known in the literature for spin-$\frac{1}{2}$ particles. Moreover, we demonstrate that the qualitative behavior of the distance-based local temperature is independent of the choice of the distance measure by comparing the trace distance, Uhlmann's fidelity and relative entropy distance. We further observe by computing local master equation that the quantum refrigerator consisting of a spin-1/2 and a spin-j particle can lead to a lower local temperature compared to a refrigerator with two identical spin-j particles following the XYZ interactions.

I. INTRODUCTION

In the last few decades, the rapidly emerging field of quantum thermodynamics [1–3] has offered the prospect for unravelling fundamental laws of miniaturized quantum systems, including thermal devices such as quantum batteries [4, 5], quantum thermal transistors [6], diodes [7] and quantum refrigerators [8]. Recent progress in quantum technologies as well as in the ability of controlling quantum systems [9–12] has fueled the experimental urge of constructing quantum thermal machines in order to see whether they outperform their classical counterparts. In this respect, it is also shown that quantum spin models, implementable in different physical substrates like cold atoms [13, 14], trapped ions [15–17], and nuclear magnetic resonance systems [18–20], can serve as important platforms to realize these quantum thermal machines [21–26].

The main task of a quantum refrigerator consisting of a few d-dimensional quantum mechanical subsystems coupled with local thermal baths is to decrease the temperature of a chosen subsystem in the steady state [8, 27–30]. This has so far been achieved using different combinations of qubits and qutrits [8, 25, 26, 31–33]. The available proposals till date include devices in which cooling is either performed with the help of one or more external energy source(s) [28], or in a self-contained fashion [8]. To obtain the minimum possible steady-state temperature, cooling assisted by various means, such as solar energy [34], rapid measurement [35], repeated collision [36], periodically modulated interactions [37], and paradigmatic quantum spin Hamiltonians [25, 26] have been reported, and even achievement of Carnot efficiency in a two-qubit setup via a reverse-coupling mechanism has been shown [38]. Moreover, recent experimental realizations of refrigerators using trapped ions [39] and several experimental proposals employing superconducting qubits [40], quantum dots [41], trapped ions [42], and optomechanical systems [43] have made the implementation of a spin model-based fridge in laboratories a possibility.

As of now, most of the proposed and implemented quantum technologies typically involve two-dimensional systems due to (a) the relative ease of handling a single or a multiqubit system compared to a system involving qudits, and (b) the fact that a quantum system moves towards the classical limit with an increase in the spin quantum numbers of the constituent spins, thereby eventually losing its quantum characteristics. However, higher dimensional quantum systems are revealed to be advantageous over their lower dimensional counterparts in several quantum gadgets, including quantum key distribution [44], quantum switch [45], and quantum batteries [46–48], to name a few. While there has been a few attempts in constructing quantum refrigerators using constituent quantum systems with a Hilbert space dimension higher than that of a qubit or a qutrit [34, 49–51], to the best of our knowledge, realization of quantum refrigerators using quantum spin models constituted of particles with arbitrary spin-quantum number remains an unexplored area, which we address in this work.

Our design of the quantum refrigerator bears two distinct features. (a) We employ interacting quantum spin systems with nearest-neighbor interactions, namely the quantum XYZ model [52] and the bilinear-biquadratic (BB) model [53–57], consisting of two or three spins having spin quantum number j. (b) In order to quantify the performance of the refrigerator, we introduce a definition of local temperature for a spin-j system that uses the minimum distance between the time-evolved state of the system and a canonical thermal state. We prove that the introduced measure reduces to the measure of local temperature based on population of the ground state in case of spin-1/2 systems that is already available in literature [8]. We further demonstrate that the proposed definition of local temperature is independent of the choice of the distance measure, by considering the trace distance, the relative entropy distance [58] and Uhlmann's fidelity [59].

We derive the explicit forms of the Lindblad operators corresponding to subsystems with spin quantum number j, when the quantum master equation is constructed following a local approach. We show, by solving the local quantum master equation, that a two- and a three-spin system of identical spins with spin-j governed by the XYZ type, or the bilinear-biquadratic interactions and connected to local bosonic thermal baths can serve as a refrigerator for a chosen spin in the
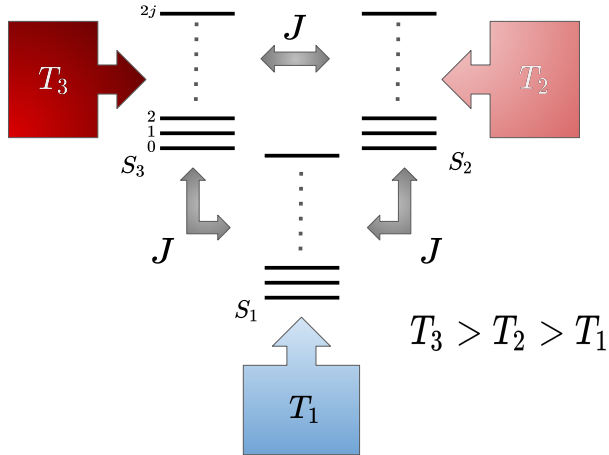
FIG. 1. (Color Online.) **Schematic representation of a quantum refrigerator consisting of three spin-j particles.** Each of the spin is coupled with non-interacting thermal baths having temperature T_1, T_2 and T_3. J is the interaction strength between the spins.

system. The performance of the refrigerator, as quantified by the proposed distance-based local temperature and the normalized von Neumann entropy of the steady state of the cold spin, exhibits diminution with an increase in j, demonstrating the dimensional advantage. We also show that a duo of a spin-$\frac{1}{2}$ and a spin-j system cooling the spin-$\frac{1}{2}$ particle has better dimensional benefit compared to a system of two identical spin-j particles with local master equation. The dimensional improvement is found to persist even when one considers the global approach of constructing the quantum master equation.

The paper is organised as follows. The setup of the refrigerator with spin models, local thermal baths, and their interactions, as well as the derivation of Lindblad operators for local quantum master equations are described in Sec. II. In Sec. III, we introduce the concept of quantifying local temperature using distance measures, and prove that it coincides with the population-based definition of local temperature for spin-1/2 systems. We also discuss the use of von Neumann entropy as an indicator for local temperature. The performance of the refrigerators constituted of two spins using these figures of merit is reported in Sec. IV. The analysis on the refrigerator with three spin-j particles is carried out in Sec. V, while we conclude in Sec. VI.

II. DESIGN FOR QUANTUM REFRIGERATOR

In this section, we briefly discuss the system-environment setup, a part of which acts as a quantum refrigerator for the rest under specific conditions of the system as well as the system-environment interaction parameters. For local master equation, we also derive the Lindblad operators applicable in higher dimensions.

A. Small spin clusters as system

We use small clusters of particles with specific types of two-body interactions to design the refrigerator, where the individual particles can take half-integer as well as integer spins. The total Hamiltonian $H_{sys} = H_{loc} + H_{int}$ of the system consists of two parts – (a) the local Hamiltonian H_{loc} given by

$$H_{loc} = \sum_{r=1}^{N} h_r S_r^z, \tag{1}$$

and (b) the interaction Hamiltonian H_{int} governed by the spin-spin interactions. We particularly focus on two types of spin-spin interactions, namely, the nearest neighbor XYZ interaction giving rise to the Hamiltonian [52]

$$H_{xyz} = J \sum_{r=1}^{N} \left[(1+\gamma) S_r^x S_{r+1}^x + (1-\gamma) S_r^y S_{r+1}^y \right]$$
$$+ J\Delta \sum_{r=1}^{N} S_r^z S_{r+1}^z, \tag{2}$$

and the bilinear-biquadratic Hamiltonian [53–57]

$$H_B(\phi) = J\cos\phi \sum_{r=1}^{N} \vec{S}_r \cdot \vec{S}_{r+1} + J\sin\phi \sum_{r=1}^{N} (\vec{S}_r \cdot \vec{S}_{r+1})^2, \tag{3}$$

where we assume periodic boundary conditions unless otherwise mentioned. Here, S_r^ν ($\nu = x, y, z$) are the $(2j+1)$ dimensional spin matrices (for a spin-j particle, $j = \frac{1}{2}, 1, \frac{3}{2}, \cdots$) acting on the site r, and N is the total number of particles in the system. The rth spin in the system is subject to a magnetic field of strength h_r in the z-direction. When the interaction is of the XYZ type, J is the strength of the spin-spin interaction strength between the nearest-neighbor spins, while γ and Δ represent the xy- and the z-anisotropy parameters respectively. When $\Delta = 0$ and $\gamma = 0$, the Hamiltonian represents the XX model while $\gamma = 0$, and $\Delta \neq 0$ gives the XXZ mmodel. On the other hand, $J\cos\phi$ and $J\sin\phi$ are the interaction strengths for the linear and the quadratic terms in the BB Hamiltonian respectively, where the parameter ϕ governs the phases of the system in the absence of the local magnetic field [53–57]. With the aim of designing small quantum thermal machines and investigating the effect of a change in the Hilbert space dimension of the system on the performance of the machine, we typically restrict the values of N to be $N = 2$ and $N = 3$.

Note that in Eqs. (2) and (3), we assume all the particles in the interacting quantum spin model to have identical spin value j. However, in a more general situation, one may consider different spin values for different particles at different lattice sites. An example of such cases will be discussed in Sec. IV B for $N = 2$.

B. Interaction with local bosonic baths

Consider a situation where each spin r in the system is interacting with a local bath B_r, $r = 1, 2, ..., N$ (see Fig. 1 for an illustration with $N = 3$), which is a collection of harmonic oscillators, described by the bath Hamiltonian

$$H_{B_r} = \int_0^{\omega_c} d\omega a_\omega^\dagger a_\omega, \tag{4}$$

so that the total bath Hamiltonian for N baths is given by $H_B = \sum_{r=1}^N H_{B_r}$. Here, a_ω ($a_\omega^\dagger$) is the annihilation (creation) operator of the mode ω, such that $[a_\omega, a_{\tilde{\omega}}^\dagger] = \delta(\omega - \tilde{\omega})$, and ω_c is the cut-off frequency of the bath. We consider the absolute temperature of the bath B_r to be T_r^0, and the baths are local in the sense that the bath B_r affects only the spin r in the entire bath-environment setup. The Hamiltonian defining the interaction between the systems and baths, denoted by H_{SB}, reads as

$$H_{SB} = \sum_{r=1}^N \sum_\omega \left(S_r^+ \otimes a_\omega + S_r^- \otimes a_\omega^\dagger \right), \tag{5}$$

where S_r^+ (S_r^-) is the spin raising (lowering) operators of rth spin, given by $S_r^\pm = S_r^x \pm iS_r^y$.

We consider a scenario where at $t = 0$, $H_{sys} = H_{loc}$, such that each spin is in thermal equilibrium with its respective bath and has an initial temperature equal to the bath temperature T_r^0, such that the initial ($t = 0$) state of the rth spin is represented by a diagonal density matrix ρ_r^0. In the eigenbasis of S_r^z having eigenvalues $j, j - 1 \ldots - j$, it takes the form as

$$\rho_r^0 = \tau_r^{2j}(0) |2j\rangle\langle2j| + \tau_r^{2j-1}(0) |2j - 1\rangle\langle2j - 1| + \cdots + \tau_r^0(0) |0\rangle\langle0|, \tag{6}$$

where

$$\tau_r^\mu(0) = \frac{\exp(-\mu\beta_r^0 h_r)}{\sum_{\mu=0}^{2j} \exp(-\mu\beta_r^0 h_r)} \tag{7}$$

with $\sum_{\mu=0}^{2j} \tau_r^\mu(0) = 1$, such that the initial state of the N-spin system is $\rho(0) = \bigotimes_{r=1}^N \rho_r^0$, and $\beta_r^0 = 1/k_B T_r^0$, k_B being the Boltzmann constant, which is set to 1. After the interaction Hamiltonian H_{int} is turned on at $t > 0$ such that $H_{sys} = H_{loc} + H_{int}$ at $t > 0$, the time-dynamics of the system is governed by the quantum master equation (QME) [60], given by

$$\dot{\rho} = -i[H_{sys}, \rho] + \mathcal{L}(\rho), \tag{8}$$

where $\mathcal{L}(.)$ represents the dissipator, emerging out of the spin-bath interactions. The solution of Eq. (8) provides the state, $\rho(t)$, of the system as a function of t.

C. Dissipators: local vs. global

There exists two competing approaches to determine the dissipator in the QME (Eq. (8)) – (a) a global approach, where transitions between the eigenstates of the entire system represented by the Hamiltonian H_{sys} is considered, and (b) a local treatment of the quantum master equation, considering only the transitions between the eigenstates of the individual subsystems labelled by $r = 1, 2, \cdots, N$. In the former, the dissipator $\mathcal{L}(\rho) = \sum_{r=1}^N L_r(\rho)$, with

$$L_r(\rho) = \sum_{\omega>0} \gamma_r(\omega) \left[\left(A_r(\omega)\rho A_r^\dagger(\omega) + A_r^\dagger(\omega)\rho A_r(\omega) \right) - \frac{1}{2} \left(\{A_r^\dagger(\omega)A_r(\omega), \rho\} + \{A_r(\omega)A_r^\dagger(\omega), \rho\} \right) \right], \tag{9}$$

where the operators $A_r(\omega)$ are the Lindblad operators corresponding to the rth spin for a transition amounting energy ω among the energy levels of the system, defined by the equation

$$e^{iH_{sys}t} \left(S_r^+ + S_r^- \right) e^{-iH_{sys}t} = 2\sum_\omega A_r(\omega)e^{-i\omega t}. \tag{10}$$

Explicit forms of $A_r(\omega)$ can be derived by decomposing the spin-part of the system-bath interaction Hamiltonian in the eigenbasis of H_{sys}, and may not always be analytically derivable in cases of complex Hamiltonians with large number of spins. The transition rate, represented by $\gamma_r(\omega)$, corresponds to the jump through an energy gap ω for the spin r, and depends on the spectral function and the cut-off frequency of the bath. For baths with an Ohmic spectral function $\kappa_r(\omega) = [\exp(\beta_r\omega) - 1]^{-1}$ and a cut-off frequency ω_c which

are the same across baths,

$$\gamma_r(\omega) = f_r(\omega)[1 + \kappa_r(\omega)], \text{ for } \omega \geq 0,$$
$$\gamma_r(\omega) = f_r(|\omega|)\kappa_r(|\omega|), \text{ for } \omega < 0, \tag{11}$$

with $f_r(\omega) = \alpha_r\omega \exp(-\omega/\omega_c)$, and α_r being a constant for the rth bath, representing the spin-bath interaction strength. Under Markovian approximation, $\max\{\alpha_r\} \ll 1$.

The explicit form of the Lindblad operators can, however, be determined if one takes a local approach for deriving the QME. Note that in the limit where the spin-spin and the spin-bath interaction strengths are so small that $H_{sys} \approx H_{loc}$ ($\gamma_r(\omega), J << h_r$), one may calculate the Lindblad operators using the eigenstates of H_{loc} only, which we present in the following for the systems consisting of spin-j particles .

Lindblad operators for spin-j local QME. Let us demon-

strate the explicit form of the Lindblad operators considering a system of two spin-j particles ($r = 1, 2$), subject to magnetic fields of strength h_1 and h_2 in the z-direction. Eigenvalues of the local Hamiltonian (Eq. (1)) for this system can be written as $(-j + a)h_1 + (-j + b)h_2$, corresponding to eigenstates $|a\rangle \otimes |b\rangle$, where $a, b \in [0, 2j]$. Writing the system-bath interaction Hamiltonian as

$$H_{SB} = \sum_{r=1}^{2} \sum_{\omega} \left[S_r^x \otimes (a_\omega + a_\omega^\dagger) + S_r^y \otimes \mathrm{i}(a_\omega - a_\omega^\dagger) \right], \tag{12}$$

the Lindblad operators corresponding to the rth bath can be determined as [60]

$$A_r(\omega) = \sum_{\epsilon_q - \epsilon_p = \omega} |\epsilon_p\rangle\langle\epsilon_p| S_r^x |\epsilon_q\rangle\langle\epsilon_q|, \tag{13}$$

where ϵ_p (ϵ_q) is the pth (qth) eigenstates of H_{loc}. Performing algebra for spin-j particles corresponding to the first spin leads to

$$A_1(\omega) = \sum_{\epsilon_q - \epsilon_p = \omega} \frac{1}{2} [\sqrt{j(j+1) - a(a+1)} |a'\rangle \langle a| \delta_{a',a+1} $$
$$+ \sqrt{j(j+1) - a(a-1)} |a'\rangle \langle a| \delta_{a',a-1}] \otimes |b\rangle \langle b|, \tag{14}$$

where $A_2(\omega)$ can also be determined with similar calculation. Considering (a) only transitions with positive ω implying $\omega = h_1$, and noticing that (b) non-zero matrix elements for $A_1(\omega)$ requires transitions to be within consecutive energy levels only, $a \in [1, 2j]$, $b \in [0, 2j]$, and $a' = a - 1$. Therefore, the desired Lindblad operator can be represented as

$$A_1(\omega) = \frac{1}{2} \left[\sum_{a=1}^{2j} \sqrt{j(j+1) - a(a-1)} |a-1\rangle\langle a| \right]$$
$$\otimes \left[\sum_{b=0}^{2j} |b\rangle\langle b| \right]$$
$$= \frac{1}{2} (S_1^- \otimes \mathbb{I}), \tag{15}$$

where $\mathbb{I}$ is the identity operator in the Hilbert space of a spin-j particle. This calculation can be extended to a system of N spin-j particles also, where the Lindblad operators for the rth bath are given by

$$A_r(\omega) = \frac{1}{2} \mathbb{I} \otimes \cdots S_r^- \otimes \ldots \mathbb{I},$$
$$A_r^\dagger(\omega) = \frac{1}{2} \mathbb{I} \otimes \cdots S_r^+ \otimes \ldots \mathbb{I}. \tag{16}$$

In this paper, we consider both local as well as global approach for constructing the Lindblad operators. However, it is important to note that unlike the global QME, the local QME may not always be appropriate for determining the non-equilibrium properties of the system due to a potential violation of second law of thermodynamics [61], and therefore

should always be used carefully. Note also that in the case of the local approach, the time-evolution of the state of a system of identical spins depends on the initial state of the system, as presented in the following proposition.

Proposition I. *For a system of identical spins, if*

$$\frac{h_r}{T_r^0} = constant \quad \forall\, r = 1, 2, \cdots, N, \tag{17}$$

the system does not evolve with time as long as the dynamics if governed by a local quantum master equation.

Proof. To prove it, we first note that $\rho(t + \delta t)$, with δt being the small increment in time, can be expanded as

$$\rho(t + \delta t) = \rho(t) + \frac{\partial\rho}{\partial t}\bigg|_t \delta t + \mathcal{O}(\delta t^2). \tag{18}$$

Performing the expansion about $t = 0$, and neglecting higher order terms, we obtain

$$\rho(\delta t) \approx \rho(0) + \frac{\partial\rho}{\partial t}\bigg|_{t=0} \delta t$$
$$= \rho(0) - \mathrm{i}[H_{sys}, \rho(0)] - \mathcal{L}(\rho(0)). \tag{19}$$

Since the interaction between the spins is absent at $t = 0$, for dissipators constructed of Lindblad operators of the form given in Eq. (16), $\mathcal{L}(\rho(0)) = 0$. Also, at $t = 0$, the condition in Eq. (17) suggests identical initial states for all spins in the system, implying $[H_{sys}, \rho(0)] = 0$, leading to $\frac{\partial\rho}{\partial t}\big|_{t=0} = 0$. This can be continued for an arbitrary small time increment δt such that $t = n\delta t$, n being an integer, when $\rho(t) = \rho(n\delta t) = \rho(0)$. Therefore, there is no time-evolution of the state in the system and the proof. $\square$

III. QUANTIFYING LOCAL TEMPERATURE IN HIGHER DIMENSION

To assess the performance of the quantum refrigerator described in Sec. II, we propose a definition of local temperature which remains valid for arbitrary spins. In this paper, we shall focus on the scenario where one aims to cool a chosen spin in the spin-bath setup during the dynamics. The rth spin in the system is said to achieve a *local steady-state cooling* by virtue of the dynamics of the system if and only if $T_r^0 > T_r^s$, where $T_r^s = T_r(t \to \infty)$ is the local steady-state temperature of the rth spin. Note that the chosen spin-bath interaction (see Sec. II B) ensures a diagonal reduced density matrix,

$$\rho_r(t) = \mathrm{Tr}_{\substack{j,k(\neq i) \\ j,k=1,2,3}} [\rho(t)], \tag{20}$$

for the rth spin. In the case of a system having a spin-$\frac{1}{2}$ particle at the rth site, we know that $\rho_r(t)$ takes the form as

$$\rho_r(t) = \tau_r^0(t) |0\rangle\langle 0| + \tau_r^1(t) |1\rangle\langle 1|, \tag{21}$$

where $\tau_r^0(t)$ ($\tau_r^1(t)$) can be identified as the time-dependent population of the state $|0\rangle$ ($|1\rangle$), and can be used to define a

population-based local temperature (PLT) for the rth spin as a function of time, given by

$$T_r(t) = \frac{h_r}{\ln\left[\tau_r^1(t)^{-1} - 1\right]}. \tag{22}$$

While this protocol for defining the local temperature of a spin-$\frac{1}{2}$ particle is well-established [8], the definition of a local temperature remains a scarcely explored area with little literature [62] (cf. [50, 51]), when the subsystems have Hilbert space dimension larger than 2 (eg. spin-j particles). In the latter situation, the local density matrix of the rth spin, having the form

$$\rho_r(t) = \tau_r^{2j}(t)\,|2j\rangle\langle 2j| + \tau_r^{2j-1}(t)\,|2j-1\rangle\langle 2j-1| + \cdots + \tau_r^0(t)\,|0\rangle\langle 0|, \tag{23}$$

depends on a total of $2j$ parameters, and hence defining a *unique* local temperature for the rth spin-j particle following the protocol for spin-$\frac{1}{2}$ particles [8] is not possible. In this regard, we put forward a distance-based quantifier for local temperature in the subsequent subsections, and justify its importance in the context of investigating performance of a quantum refrigerator constructed out of quantum spin models. In this way, a set of definition for local temperature emerges depending on the choice of valid distance measures although we show that they qualitatively behave in a similar fashion.

A. Estimating local temperature using distance measures

Let us consider an arbitrary canonical thermal state of the rth spin-j particle in the system, having an absolute temperature T_r'. The canonical thermal state is given by

$$\tilde{\rho}_r = \frac{\exp(-\beta_r' h_r S_r^z)}{\mathrm{Tr}\left[\exp(-\beta_r' h_r S_r^z)\right]}, \tag{24}$$

where $\beta_r' = 1/k_B T_r'$ is the inverse temperature, and h_r is the strength of the external magnetic field of the rth spin. We define the *distance-based local temperature* (DLT), $T_r^D(t)$, for the rth spin described by the steady state $\rho_r(t)$ obtained via the dynamics (see Eq. (23)) as

$$T_r^D(t) = \frac{1}{\min\limits_{T_r'} D(\tilde{\rho}_r, \rho_r(t))}, \tag{25}$$

where $D(\tilde{\sigma}, \sigma)$ is an appropriate distance measure between the density matrices $\tilde{\sigma}$ and σ. There exists a number of distance measures in literature, including the trace distance [58], the Hilbert-Schmidt distance [63], Uhlmann fidelity [59, 64], and the relative entropy distance [65] to name a few, which can be used to quantify the local temperature, and the use of a particular measure may depend on specific situations. In the following sections, we shall compare the performances of different distance measures in context of faithfully quantifying the local temperature of a spin-j system. In order to justify the importance of such a definition of local temperature, we present the following proposition.

■ **Proposition II.** *For a spin-$\frac{1}{2}$ particle, the distance-based local temperature is equivalent to the population-based local temperature at all times, when trace distance is chosen as the distance measure.*

Proof. Let us define

$$y_r = \frac{\exp(-\beta_r' h_r/2)}{\exp(-\beta_r' h_r/2) + \exp(\beta_r' h_r/2)}, \tag{26}$$

and write $D(\tilde{\rho}_r, \rho_r(t))$, at an arbitrarily fixed time instant t, as a function of y_r as

$$D(y_r) = \frac{1}{2}\mathrm{Tr}\sqrt{(\tilde{\rho}_r - \rho_r(t))^\dagger(\tilde{\rho}_r - \rho_r(t))}$$
$$= \frac{1}{2}\left(|y_r - \tau_r^1(t)| + |(1-y_r) - \tau_r^0(t)|\right), \tag{27}$$

which, using $\tau_r^0 = 1 - \tau_r^1$, becomes

$$D(y_r) = \frac{1}{2}\left(|y_r - \tau_r^1(t)| + |\tau_r^1 - y_r|\right). \tag{28}$$

Since $D(y_r) \geq 0$ by virtue of being a distance measure, and $D(y_r) = 0$ for $y_r = \tau_r^1$, the DLT is obtained from the equation $y_r = \tau_r^1$ by solving for T_r' as

$$T_r' = \frac{h_r}{\ln\left[\tau_r^1(t)^{-1} - 1\right]}. \tag{29}$$

Since Eq. (29) holds for an arbitrary t, the DLT is equivalent to the PLT at all times. Hence the proof. □

In the subsequent sections, we shall discuss the steady-state cooling of a spin in the system using DLT as a quantifier for cooling, where for brevity, we denote the steady-state DLT as $T_r^s = T_r^D(t \to \infty)$.

B. Entropy-based estimation of local temperature

In situations where a spin-j subsystem of a quantum spin model in a system-bath setup described in Sec. II attains a local steady-state cooling, the entropy of the subsystem in the steady state should be lower than the initial entropy of the subsystem at $t = 0$, providing a signature of the cooling phenomena. In order to carry out a quantitative investigation, we define an entropy-based estimated temperature, quantified by the normalized entropy for the steady state, as

$$S_N^s = \frac{S(\rho_r(t \to \infty))}{S(\rho_r(0))}, \tag{30}$$

where $S(\rho) = -\mathrm{Tr}(\rho \log_2 \rho)$ is the von Neumann entropy for the density matrix ρ. A local steady-state cooling of the rth spin is indicated by $S_N^s < 1$ while its positivity implies heating. The qualitative variations of S_N^s as functions of the relevant system parameters as well as with increasing dimension of the Hilbert spaces of the subsystems are similar to those for DLT, as we shall demonstrate in the subsequent sections.
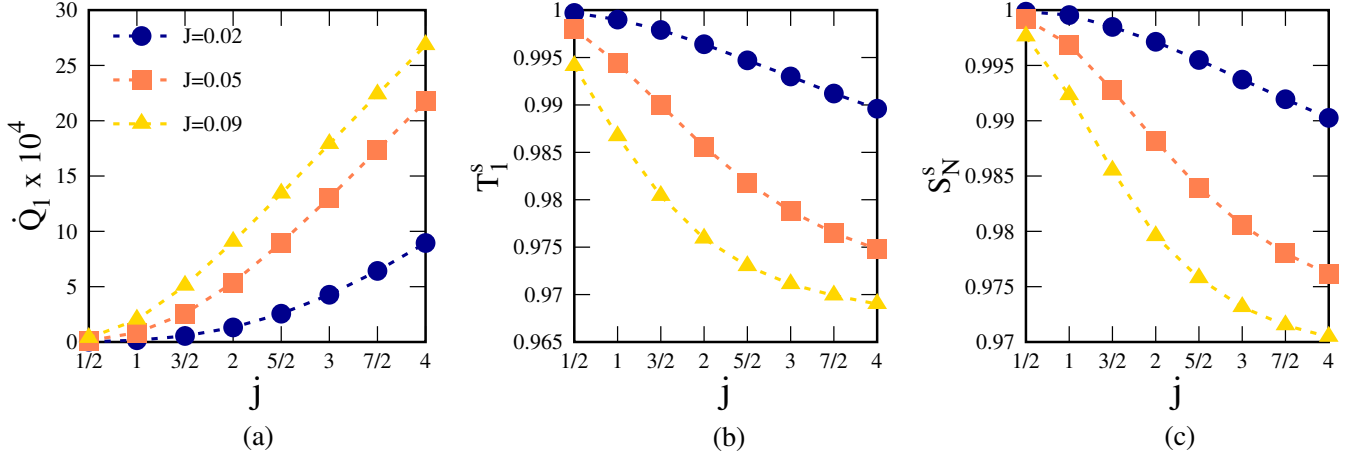
FIG. 2. (Color online.) **Variation of (a) heat current, (b) steady-state temperature and (c) normalized von-Neumann entropy (vertical axis) as functions of the dimension of the first subsystem, j (horizontal axis).** The refrigerator consists of two identical spins which are interacting according to the XX Hamiltonian given in Eq. (2) with $\gamma = 0$ and $J\Delta = 0$. We compute these quantities by solving local QME. Circles, squares and triangles represent different interaction strengths, namely $J = 0.02$, $J = 0.05$ and $J = 0.09$ respectively. The local external magnetic fields of the first and the second spins are respectively $h_1 = 1.1$, and $h_2 = 1.3$ while the corresponding initial temperature of the first and the second spins are $T_1(0) = 1$ and $T_2(0) = 1.1$ respectively. Here the spin-bath interaction is chosen as $\Gamma = 0.05$. The dimensional advantage according to the figures of merit for the refrigerator is clearly visible. All the axes are dimensionless.

C. Local heat current

An important quantity, providing the indication as to whether an N-spin system is operating as a refrigerator for the rth spin, is the local heat current at the steady state, defined as [60]

$$\dot{Q}_r = \text{Tr}\left[H_{sys}\mathcal{L}_r(\rho^s)\right], \tag{31}$$

where ρ^s is the steady state $\rho(t \to \infty)$ of the entire system. A positive value of $\dot{Q}_r$ represents a situation where heat flows from the bath B_r to the rth spin in the steady state, which is at a lower temperature $T_r^s < T_r^0$ if a steady-state cooling has been achieved. The value of $\dot{Q}_r$, therefore, is expected to be positive in accordance with a cooling indicated by $T_r^{D,s}$ and S_N^s. Note, however, that the definition of H_{sys} may vary depending on the choice of a local, or a global approach to define the QME, and an inappropriate choice of the QME may lead to anomalous values of $\dot{Q}_r$, although the steady-state cooling for the rth spin is indicated by the values of $T_r^{D,s}$ and S_N^s [26, 66]. We shall elaborate on this in the subsequent sections as we discuss specific constructions of small refrigerators in a case-by-case basis.

IV. TWO-SPIN QUANTUM REFRIGERATORS

We now discuss the performance of quantum refrigerators built with two spins, where one of the spins is cooled and the other spin, along with the baths, constitute the refrigerator. Unless otherwise mentioned, in the rest of the paper, we always choose the first spin, i.e., $r = 1$ to be the target spin for cooling.

A. System of two identical spins

Let us consider two identical interacting spin-j particles constituting the system, and increase the value of j simultaneously for both the spins to study how the refrigeration of one of the spins depends on j. Unless otherwise mentioned, in all our analysis, we use the trace distance to define the DLT. For computing heat current, local temperature and entropy, we solve the local as well as global QME using the Runge-Kutta fourth order technique, and determine the reduced state of the spin-j particle in the steady state that is used to compute the relevant quantities.

Tuning refrigerator with system parameters

XYZ **model as refrigerator.** We first consider the XYZ-type interaction between the spins, and solve the time-dependent state of the system using the local QME to compute $\dot{Q}_1$, T_1^s, and S_N^s corresponding to the first spin. Fig. 2 depicts the variations of these quantities as a function of j, clearly indicating significant advantage in cooling of the first spin when the dimension of the Hilbert spaces corresponding to the spins increases. For example, with $J = 0.09$, in case of spin-$1/2$, the decrease in temperature at the steady state from the initial state is $\approx 0.59\%$ while it is 3.1% for the refrigerator with spin-4 systems. Also, our results indicate that a higher value of J favours the cooling of the first spin, compared to a lower value. In our analysis, we have kept the value of J to be in such a range that the local QME can be applied. However, the improvement in cooling for higher values of J indicates the need for an investigation with the global QME, which we
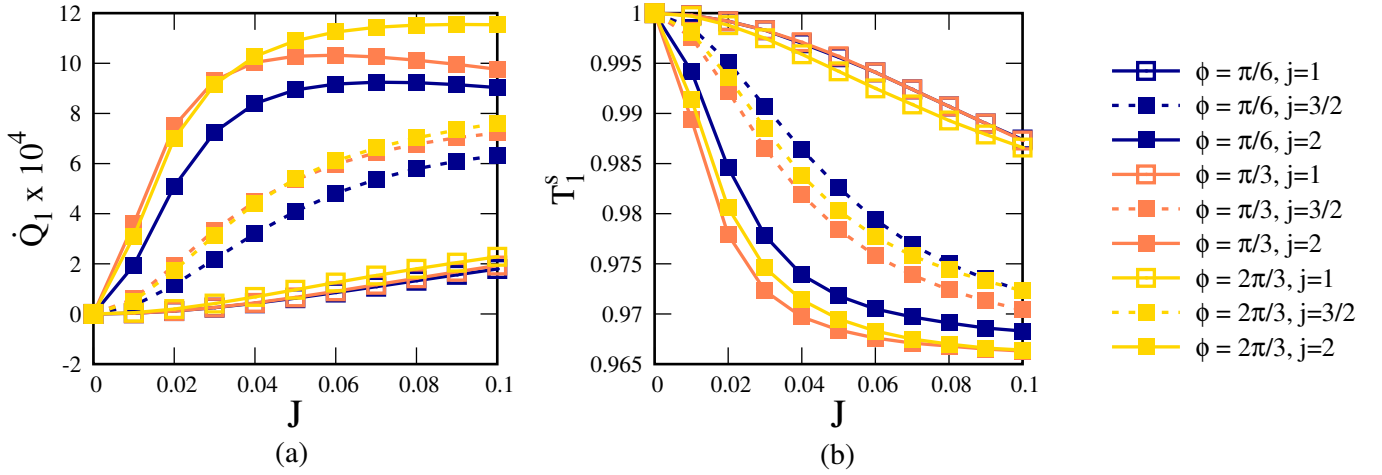
FIG. 3. (Color online) Trends of (a) heat current and (b) local temperature in the steady state (vertical axis) against the interaction strength, J for BB Hamiltonian (horizontal axis). Hollow squares with solid line, solid squares with dashed line and solid squares with solid line respectively represent $j = 1, 3/2$ and 2 respectively while blue, orange and yellow respectively denotes the phases, $\phi = \pi/6, \pi/3$ and $2\pi/3$. All other specifications are same as Fig. 2. All the axes are dimensionless.
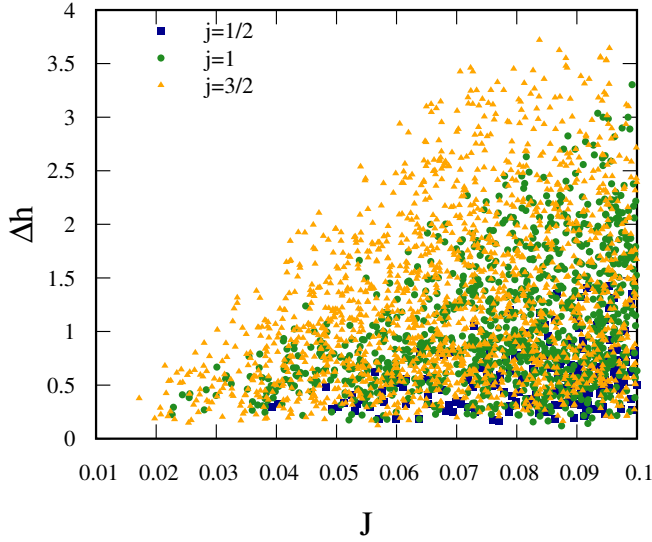
FIG. 4. (Color online.) Scattered plot of the steady-state temperature only when cooling occurs in the $(J, \Delta h = h_2 - h_1)$-plane. Squares, circles and triangles represent respectively $j = 1/2, 1$ and $3/2$. Other specifications are same as Fig. 2. Among 7×10^3 choices of parameters of the refrigerator based on the XX model, 2.7%, 14.3% and 23.82% of situations are found to exhibit cooling in the steady state with $j = 1/2$, $j = 1$ and $j = 3/2$ respectively. Both the axes are dimensionless.

shall discuss in the subsequent subsections.

Note that the results presented in Fig. 2 is for the case of $\gamma = 0$ and $\Delta = 0$, representing the XX Hamiltonian. Our data suggests that even in the presence of the xy- and the z-anisotropy in the interaction, the dimensional advantage in cooling persists although the variation of the relevant quantities is almost negligible with non-zero values of the anisotropies for a fixed value of j, especially with low j val-

ues. For high j, the slight change in the local temperature happens with the introduction of γ and Δ and the results suggest that the performance of the refrigerator based on the XXZ model is the best among the class of XYZ models. Therefore, the behaviors of the heat current, entropy and local temperature depicted in Fig 2 faithfully capture all the relevant information regarding the effect of increasing spin-dimension and the spin-spin interaction strength on performance of the refrigerator. Note that the positive or negative coupling strength, J, leads to the same local temperature in the steady state.

Refrigerator with bilinear-biquadratic interactions. Using the local approach, we also investigate the performance of the two-spin refrigerator when the spin-spin interactions are governed by the BB Hamiltonian (see Fig. 3), and have found the results to be qualitatively similar to that reported in Fig. 2. The dimensional advantage of cooling is present irrespective of the phase of the system from which the spin-spin interaction parameter is chosen. Specifically, the parameters chosen for demonstration reveals that the minimum temperature is obtained when the corresponding system at equilibrium belongs to the critical phase.

Note. A comment on the choice of the system parameters for the demonstration of refrigeration is in order here. Although numerous points in the parameters space of the system parameters exists where a local steady-state cooling for the first spin is observed, the total volume of the parameter space that represents such refrigerators is small compared to the entire parameter space although it increases with the increase of the spin-dimension. In Fig. 4, we depict, for $j = \frac{1}{2}, 1, \frac{3}{2}$, the points in the parameter space of J and $\Delta h = h_2 - h_1$ for which a steady-state cooling of at least $T_1^0 - T_1^s = 10^{-3}$ is obtained. The fraction of points representing a refrigerator increases with an increase in j 2.7%, 14.3% and 23.82% for $j = 1/2$, 1, and $3/2$ respectively, demonstrating again a dimensional advantage in the accessibility of parameter space in building a quantum refrigerator. Note also the higher clus-
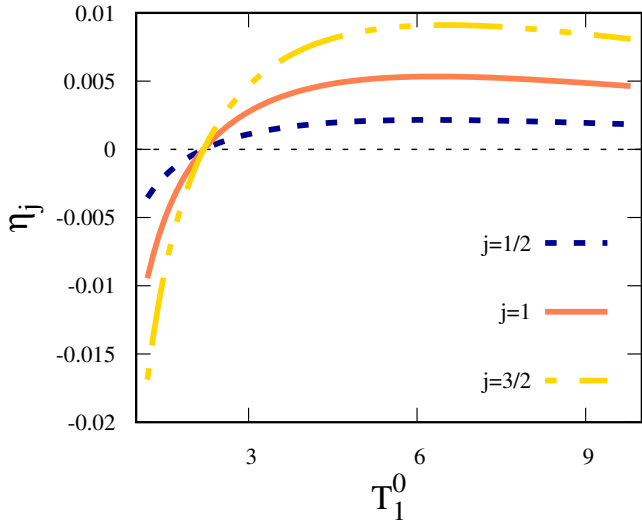
FIG. 5. (Color online) Dependence of steady state cooling factor, η_j (vertical axis) vs. initial temperature (horizontal axis). Dashed, solid and dotted lines represent spin quantum number, $j = 1/2$ 1 and 3/2 respectively. Here $J = 0.05$ and $T_2^0 - T_1^0 = 0.4$. Other specifications are same as in Fig. 2. Both the axes are dimensionless.
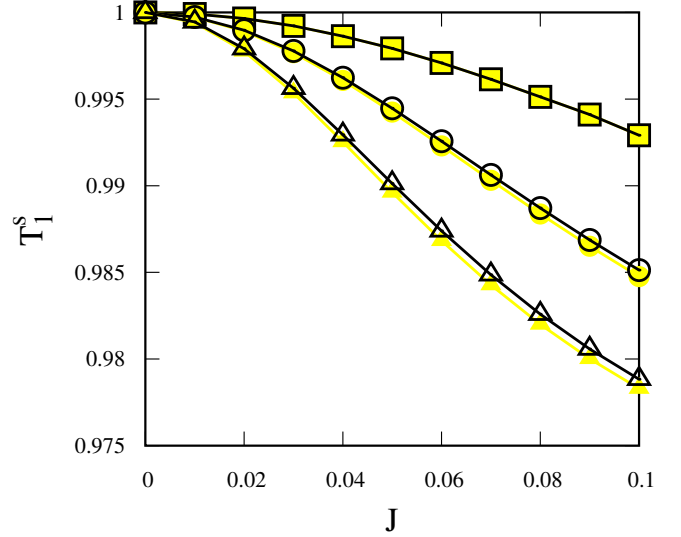

FIG. 6. (Color online) Behavior of steady-state local temperature of the target spin obtained via trace and relative entropy distance (ordinate) with respect to interaction strength, J (abscissa). Solid and hollow symbols represent trace and relative entropy distance. Squares, circles and triangles are respectively for refrigerators with two identical spins having $j = 1/2$, 1, 3/2. Other specifications are same as Fig. 2. All the axes are dimensionless.

tering of the accessible points in parameter space towards a high value of J, indicating the need for performing a global QME-based analysis of the system. Interestingly, however, we notice that there exists a forbidden regime in the $(J, \Delta h)$-plane where the cooling with XX interactions does not occur and it decreases with dimensions.

Tuning refrigerator with bath temperature

Along with system parameters, it is also important to investigate how the performance of the refrigerator can be controlled when one has access to the tunable parameters of the thermal baths, such as the bath temperatures T_r^0. Towards this aim, we define a steady-state cooling factor relative to the initial temperature of the cold spin-j particle in the system, as

$$\eta_j = \frac{T_1^0 - T_1^s}{T_1^0}. \tag{32}$$

In Fig. 5, we plot the variation of η_j as function of T_1^0, which exhibits a critical point T_1^c on the T_1^0-axis corresponding to a zero-crossing of η_j. For $T_1^0 < T_1^c$, a steady-state heating of the first spin takes place represented by a negative value of η_j, while when $T_1^0 > T_1^c$, a positive value of η_j is obtained due to the occurrence of a steady-state cooling. Note that for the reported data, the critical point T_1^c corresponds to the situation described in Proposition I, such that

$$\frac{h_1}{T_1^c} = \frac{h_2}{T_2^0}, \tag{33}$$

ensuring that no evolution of the system takes place. Note also that our numerical analysis clearly suggests that

$$\eta_{j=\frac{1}{2}} < \eta_{j=1} < \eta_{j=\frac{3}{2}}, \tag{34}$$

thereby exhibiting the importance of higher dimensional subsystems in enhancing the performance of the designed refrigerator.

Local temperature with different distance measures. At this point, it is natural to ask whether the reported results remain invariant under a change in the choice of the distance measure used to quantify the DLT. We answer this question affirmatively. Fig. 6 depicts a comparison between the DLT values obtained by using the trace distance and the relative entropy distance, defined as $S(\sigma_1 || \sigma_2) = \text{Tr}[\sigma_1 \log_2 \sigma_1 - \sigma_1 \log_2 \sigma_2]$, for two density matrices σ_1 and σ_2. While the two measures provide identical results for qubit systems, the values of the DLTs differ by $\sim 10^{-3}$ with increasing j. Nonetheless, the qualitative behavior remains similar in all these situations. It is also noteworthy that the difference is very small for low values of the spin-spin interaction strength, and increases very slowly with an increase in J. We also check the performance of the DLT using Uhlmann fidelity [59] as the distance measure, which coincides with the DLT using relative entropy distance.

Refrigeration using the global QME

A question that naturally arises is to whether the results corresponding to a quantum refrigerator obtained using the local QME remains the same even in situations where a global QME is appropriate to describe the dynamics of the system. To answer this question, we find that in the case of a two-spin models described by the Hamiltonian H_{xyz}, cooling of the first spin takes place only with a non-zero value of ΔJ
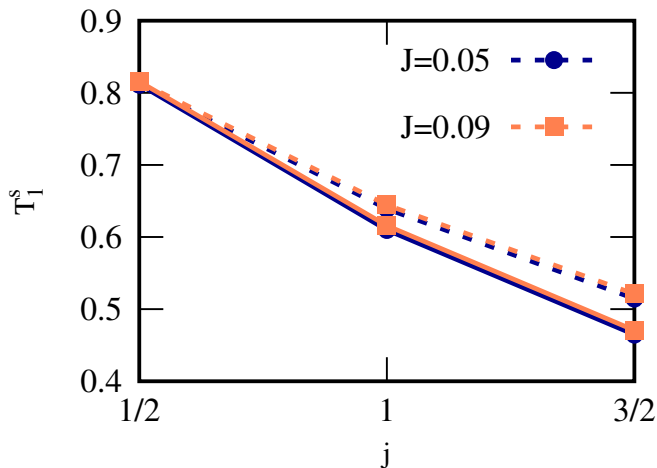
FIG. 7. (Color online) **Steady-state local temperature (ordinate) with the variation of spin quantum number j (abscissa).** The dashed line is obtained by solving global QME for the XXZ model with two identical spin-j systems and the solid line is for the refrigerator consisting of a spin-1/2 and spin-j particles. Here $J = 0.05$ (circles) and $J = 0.09$ (squares) with $J\Delta = -1.0$ while the strength of the magnetic fields and the spin-bath interactions are chosen as $h_1 = 1.1$, $h_2 = 1.3$, $\alpha_1, \alpha_2 = 10^{-3}$ and $\omega_c = 10^3$ respectively, and the initial temperatures of each spin are same as in Fig. 2. See text for the improvement obtained with global QME over the local ones. Both the axes are dimensionless.

(see Fig. 7 for a typical cooling phenomena for the first spin). This is in stark contrast with the situations discussed so far involving the local QME, where the zz-interaction term in H_{xyz} does not have any significant effect on cooling (cf. [26]). However, even in the case of the global QME, the features like significant dimensional advantage remains unaltered, and the amount of refrigeration of the first spin is much higher in comparison to the case of the local QME. For example, for spin-1/2 systems, the percentage of cooling in the first spin is approximately 18.8% with global QME while for spin-3/2 quantum refrigerator, it is 53.5% for the XXZ model refrigerator with $J = 0.05$ and $J\Delta = -1$.

B. System of two different spins

Let us design a refrigerator with two spins having different values of j, and focus specifically on the situation where $j = \frac{1}{2}$ for the first spin ($r = 1$), while for the second spin ($r = 2$), j can take an arbitrary value. While it is known that a qubit can be cooled in a qubit-qutrit system with specific interaction between them [8], it is not yet clear whether increasing the Hilbert space dimension of the second party in a $2 \times (2j+1)$ system provides any advantage to the refrigeration of the qubit system. To address this question, we consider the Hamiltonian modelling the interaction between the spin-1/2 and spin-j particle to be

$$H_{xx} = J[\tilde{S}_1^x S_2^x + \tilde{S}_1^y S_2^y], \quad (35)$$

where $\tilde{S}$ (S) represents the spin operator corresponding to the spin-$\frac{1}{2}$ (spin-j) subsystem, and J is the strength of the spin-spin interaction. In Figs. 8(a) and (b), we respectively observe the patterns of $\dot{Q}_1$ and T_1^s of the spin-$\frac{1}{2}$ particle by varying j for the second spin. With an increasing j for the second spin, $\dot{Q}_1$ (T_1^s) starts from a low positive value and then increases (starts from a value $\approx T_1^0$ and then decreases), exhibiting again the dimensional advantage in cooling the first spin. Surprisingly, we observe that in this non-identical scenario, the minimum temperature corresponding to $j = 4$ of the second spin (i.e., the decrease of temperature, $\approx 4.82\%$) is much lower (higher) than that obtained for the scenario with identical spins (the decrease from the initial temperature, $\approx 3.1\%$ (comparing Figs. 2 and 8). We also perform the same analysis using the global QME to find a more pronounced dimensional advantage. Specifically, with the XXZ model ($J = 0.05$, $J\Delta = -1$), we find that a 18.9% cooling of the first spin in the case of $j = \frac{1}{2}$ for the second spin occurs while it becomes 48.53%, when the spin quantum number of the second spin is increased to $j = 3/2$.

V. REFRIGERATION IN THREE-SPIN SYSTEMS

Let us now move to a set up of refrigerator consisting of three identical spin-j particles, each of which is connected to a local thermal bath as shown in Fig. 1. Starting with the product state of a local Hamiltonian, H_{loc}, the system evolves according to Hamiltonian, H_{xyz} or H_B at $t > 0$. In case of the XYZ refrigerator, we consider an isotropic case ($\gamma = 0, \Delta = 0$) for demonstration of the performance of the refrigerator in a local QME approach. Fig. 9 depicts the variations of $\dot{Q}_1$, T_1^s, and S_N^s as functions of j for different values of J, clearly demonstrating a dimensional advantage. Note that although the qualitative results on refrigeration of the first spin using the three-spin system remains similar to its two-spin variant (see Sec. IV), quantitatively the two-spin refrigerator performs better than the three-spin one, which can be seen by comparing Fig. 9 with Fig. 2.

In case of refrigerator with three-spins governed by the BB Hamiltonian, T_1^s and S_N^s again exhibit increasing cooling of the first spin with increasing J as well as with the increase of spin quantum number, j. As observed for the two-spin refrigerator, the phase dependence also remains unaltered. However, the heat current, $\dot{Q}_1$ exhibits a non-monotonic variation with J for $j = 2$ when $\phi = \pi/3$ and $2\pi/3$, and becomes negative for moderate and high values of J. We point out here that we have defined the local heat current following the global approach (see Sec. II B) which may lead to such anomalous behavior in the heat current (cf. [26, 61, 66–69]).

VI. CONCLUSION

Summarizing, we have designed a quantum refrigerator built of a few spins whose individual Hilbert space dimensions can go beyond the qubits, or qutrits. The spins are considered to be interacting among each other via the XYZ and the bi-
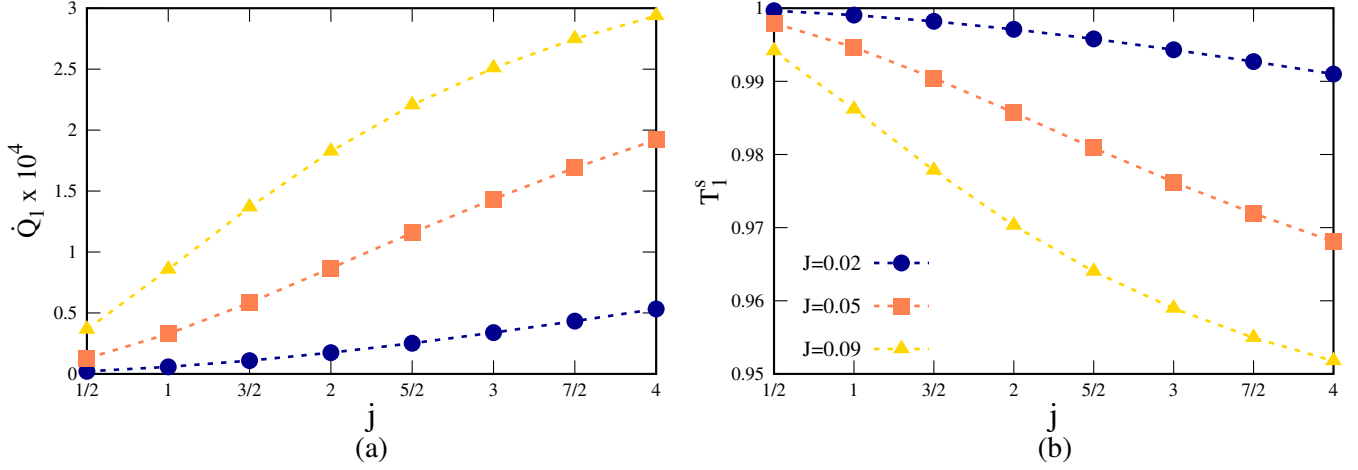
FIG. 8. (Color online) (a) $\dot{Q}_1$ and (b) T_1^s (ordinate) against the dimension, j (abscissa). Here the refrigerator is built with a spin-$1/2$ and a spin-j particles governed by the Hamiltonian H_{xx} in Eq. (35). All other specifications are same as in Fig. 2. All the axes are dimensionless.
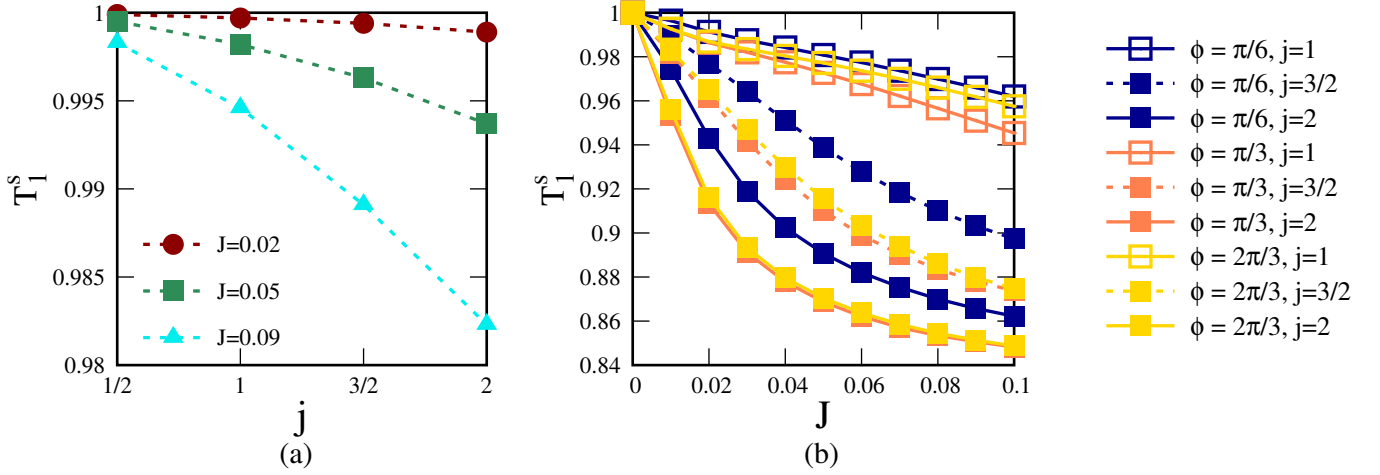

FIG. 9. (Color online) (a) Local temperature (vertical axis) as a function of the dimension of the spins j (horizontal axis) with $N = 3$ for Heisenberg XX Hamiltonian. Here we choose $h_1 = 1.5$, $h_2 = 2.5$, $h_3 = 3.5$ and $\Gamma = 0.05$, and the initial temperature of each spin is $T_1(0) = 1$, $T_2(0) = 1.1$ and $T_3(0) = 1.5$. (b) T_1^s (ordinate) against interaction strength J (abscissa) with $N = 3$ for the refrigerator based on the BB Hamiltonian for different ϕ values. Initial values of the magnetic fields, temperature and bath-system interaction strengths are same as in the XX model. All the axes are dimensionless.

linear biquadratic interactions, while each of the spins are locally interacting with the bosonic baths. So far, such machines have typically been built with spin-$1/2$ or spin-1 systems, and the quantifiers of the performances of these machines, such as definitions of local temperature for the constituent subsystems, are designed accordingly. To deal with the higher dimensional systems, in this paper, we propose a new definition of local temperature based on the minimum distance between the dynamical state of a spin-j particle in the steady state, and a canonical thermal state of the same particle, which proves to be a faithful quantifier for the performance of the designed refrigerator. The definition is proved to be consistent with the existing definitions for qubit systems, and the behavior of the

distance-based local temperature is found to be in agreement with the local heat current and the entropy of the subsystems. We observed that our setup leads to a cooling of one of the spins in the system, which enhances with the increase of the spin quantum number of the spins, and thereby with the increase of the Hilbert space dimension, hence establishing the dimensional advantage in the refrigerators. On our way to verify these results by using both local and global quantum master equations, we have also analytically derived the form of the Lindblad operators corresponding to the individual spins while constructing the dissipator for the local quantum master equation.

Miniaturisation of devices are necessary to fulfil the current

way of living. Although most of these devices work according to the laws of classical physics, they have now started knocking at the door of the quantum world due to immense advancement in the design and control of machines at the microscopic scale. In recent years, it has been established that appliances based on quantum mechanics can remarkably enhance the efficiencies compared to that obtained from the existing ones, thereby revolutionizing the world of technologies. In this respect, our work explores and manifests building small quantum refrigerators using quantum spin systems with large spins. The scope for future exploration from our work is immense. For instance, note that starting from a microscopic quantum thermal machine, there exists two routes to macroscopicity – (a) by increasing dimension of individual subsystems of a composite quantum system while keeping the number of subsystems small, and (b) by having a large number of small subsystems [30, 70]. Our results explores the former, while the latter also gained some interests in the recent past [71–76]. It will be interesting to find out the hierarchies, if any, among the macroscopic devices obtained following these two different routes.

[1] Binder.F, Correa.L.A., Andres.J, and Adesso.G, *Thermodynamics in the quantum regime,"Fundamental Theories of Physics* (SpringerBriefs in Physics, Springer, Spain, 2018).

[2] G. Gemmer, M. Michel, and G. Mahler, *Quantum Thermodynamics* (Springer, New York, 2004).

[3] S. Deffner and S. Campbell, *Quantum Thermodynamics*, 2053-2571 (Morgan and Claypool Publishers, 2019).

[4] R. Alicki and M. Fannes, Phys. Rev. E **87**, 042123 (2013).

[5] D. Ferraro, M. Campisi, G. M. Andolina, V. Pellegrini, and M. Polini, Phys. Rev. Lett. **120**, 117702 (2018).

[6] K. Joulain, J. Drevillon, Y. Ezzahri, and J. Ordonez-Miranda, Phys. Rev. Lett. **116**, 200601 (2016).

[7] J. Ordonez-Miranda, Y. Ezzahri, and K. Joulain, Phys. Rev. E **95**, 022128 (2017).

[8] N. Linden, S. Popescu, and P. Skrzypczyk, Phys. Rev. Lett. **105**, 130401 (2010).

[9] J. M. Raimond, M. Brune, and S. Haroche, Rev. Mod. Phys. **73**, 565 (2001).

[10] I. Bloch, J. Dalibard, and W. Zwerger, Rev. Mod. Phys. **80**, 885 (2008).

[11] H. Häffner, C. Roos, and R. Blatt, Physics Reports **469**, 155 (2008).

[12] J.-W. Pan, Z.-B. Chen, C.-Y. Lu, H. Weinfurter, A. Zeilinger, and M. Żukowski, Rev. Mod. Phys. **84**, 777 (2012).

[13] L.-M. Duan, E. Demler, and M. D. Lukin, Phys. Rev. Lett. **91**, 090402 (2003).

[14] M. Lewenstein, A. Sanpera, V. Ahufinger, B. Damski, A. Sen(De), and U. Sen, Advances in Physics **56**, 243 (2007), https://doi.org/10.1080/00018730701223200.

[15] F. Mintert and C. Wunderlich, Phys. Rev. Lett. **87**, 257904 (2001).

[16] D. Porras and J. I. Cirac, Phys. Rev. Lett. **92**, 207901 (2004).

[17] C. Monroe, W. C. Campbell, L.-M. Duan, Z.-X. Gong, A. V. Gorshkov, P. W. Hess, R. Islam, K. Kim, N. M. Linke, G. Pagano, P. Richerme, C. Senko, and N. Y. Yao, Rev. Mod. Phys. **93**, 025001 (2021).

[18] J. Zhang, G. L. Long, W. Zhang, Z. Deng, W. Liu, and Z. Lu, Phys. Rev. A **72**, 012331 (2005).

[19] K. R. K. Rao, H. Katiyar, T. S. Mahesh, A. Sen (De), U. Sen, and A. Kumar, Phys. Rev. A **88**, 022312 (2013).

[20] K. R. K. Rao, T. S. Mahesh, and A. Kumar, Phys. Rev. A **90**, 012306 (2014).

[21] F. Campaioli, F. A. Pollock, F. C. Binder, L. Céleri, J. Goold, S. Vinjanampathy, and K. Modi, Phys. Rev. Lett. **118**, 150601 (2017).

[22] T. P. Le, J. Levinsen, K. Modi, M. M. Parish, and F. A. Pollock, Phys. Rev. A **97**, 022106 (2018).

[23] S. Ghosh, T. Chanda, and A. Sen(De), Phys. Rev. A **101**, 032115 (2020).

[24] S. Ghosh, T. Chanda, S. Mal, and A. Sen(De), Phys. Rev. A **104**, 032207 (2021).

[25] A. Hewgill, J. O. González, J. P. Palao, D. Alonso, A. Ferraro, and G. De Chiara, Phys. Rev. E **101**, 012109 (2020).

[26] T. K. Konar, S. Ghosh, A. K. Pal, and A. Sen(De), arXiv:2107.11668 (2021).

[27] A. E. Allahverdyan, R. S. Gracià, and T. M. Nieuwenhuizen, Phys. Rev. Lett. **93**, 260404 (2004).

[28] Y. Elias, T. Mor, and Y. Weinstein, Phys. Rev. A **83**, 042340 (2011).

[29] A. E. Allahverdyan, K. V. Hovhannisyan, D. Janzing, and G. Mahler, Phys. Rev. E **84**, 041109 (2011).

[30] O. Arisoy and Ö. E. Müstecaplıoğlu, Scientific Reports **11**, 12981 (2021).

[31] M. T. Naseem, A. Misra, and Özgür E Müstecaplıoğlu, Quantum Science and Technology **5**, 035006 (2020).

[32] Y. Khlifi, A. El Allati, A. Salah, and Y. Hassouni, International Journal of Modern Physics B **34** (2020), https://doi.org/10.1142/S0217979220502124.

[33] B. Bhandari and A. N. Jordan, Phys. Rev. B **104**, 075442 (2021).

[34] J. Wang, Y. Lai, Z. Ye, J. He, Y. Ma, and Q. Liao, Phys. Rev. E **91**, 050102 (2015).

[35] N. Erez, G. Gordon, M. Nest, and G. Kurizki, Nature **452** (2008), 10.1038/nature06873.

[36] G. D. Chiara, G. Landi, A. Hewgill, B. Reid, A. Ferraro, A. J. Roncaglia, and M. Antezza, New Journal of Physics **20**, 113024 (2018).

[37] V. Cavina, P. A. Erdman, P. Abiuso, L. Tolomeo, and V. Giovannetti, Phys. Rev. A **104**, 032226 (2021).

[38] R. Silva, P. Skrzypczyk, and N. Brunner, Phys. Rev. E **92**, 012136 (2015).

[39] G. Maslennikov, S. Ding, R. Hablützel, J. Gan, A. Roulet, S. Nimmrichter, J. Dai, V. Scarani, and D. Matsukevich, Nature Communications **10**, 202 (2019).

[40] P. P. Hofer, M. Perarnau-Llobet, J. B. Brask, R. Silva, M. Huber, and N. Brunner, Phys. Rev. B **94**, 235420 (2016).

[41] D. Venturelli, R. Fazio, and V. Giovannetti, Phys. Rev. Lett. **110**, 256801 (2013).

[42] M. T. Mitchison, M. Huber, J. Prior, M. P. Woods, and M. B. Plenio, Quantum Science and Technology **1**, 015001 (2016).

[43] A. Mari and J. Eisert, Phys. Rev. Lett. **108**, 120602 (2012).

[44] T. Durt, N. J. Cerf, N. Gisin, and M. Żukowski, Phys. Rev. A **67**, 012311 (2003).

[45] K. Wei, N. Tischler, S.-R. Zhao, Y.-H. Li, J. M. Arrazola, Y. Liu, W. Zhang, H. Li, L. You, Z. Wang, Y.-A. Chen, B. C. Sanders, Q. Zhang, G. J. Pryde, F. Xu, and J.-W. Pan, Phys. Rev. Lett. **122**, 120504 (2019).

[46] A. C. Santos, B. Çakmak, S. Campbell, and N. T. Zinner, Phys. Rev. E **100**, 032107 (2019).

[47] F.-Q. Dou, Y.-J. Wang, and J.-A. Sun, EPL (Europhysics Letters) **131**, 43001 (2020).

[48] S. Ghosh and A. Sen(De), arXiv:2104.06899 (2021).

[49] L. A. Correa, Phys. Rev. E **89**, 042128 (2014).

[50] R. Silva, G. Manzano, P. Skrzypczyk, and N. Brunner, Phys. Rev. E **94**, 032120 (2016).

[51] A. Usui, W. Niedenzu, and M. Huber, Phys. Rev. A **104**, 042224 (2021).

[52] B. K. Chakrabarti, A. Dutta, and P. Sen, *Quantum Ising phases and transitions in transverse Ising models* (Springer Berlin Heidelberg, 1996).

[53] B. Sutherland, Phys. Rev. B **12**, 3795 (1975).

[54] L. Takhtajan, Phys. Lett. A **87**, 479 (1982).

[55] H. Babujian, Phys. Lett. A **90**, 479 (1982).

[56] G. Fáth and J. Sólyom, Phys. Rev. B **44**, 11836 (1991).

[57] G. Fáth and J. Sólyom, Phys. Rev. B **47**, 872 (1993).

[58] M. A. Nielsen and I. L. Chuang, *Quantum Computation and Quantum Information* (Cambridge University Press, 2009).

[59] A. Uhlmann, Reports on Mathematical Physics **9**, 273 (1976).

[60] H.-P. Breuer and F. Petruccione, *The Theory of Open Quantum Systems* (Oxford University Press, 2007).

[61] H. Wichterich, M. J. Henrich, H.-P. Breuer, J. Gemmer, and M. Michel, Phys. Rev. E **76**, 031115 (2007).

[62] P. C. Burke, G. Nakerst, and M. Haque, "Assigning temperatures to eigenstates," (2021), arXiv:2111.05083 [cond-mat.stat-mech].

[63] M. Ozawa, Physics Letters A **268**, 158 (2000).

[64] R. Jozsa, Journal of Modern Optics **41**, 2315 (1994), https://doi.org/10.1080/09500349414552171.

[65] P. E. M. F. Mendonça, R. d. J. Napolitano, M. A. Marchiolli, C. J. Foster, and Y.-C. Liang, Phys. Rev. A **78**, 052330 (2008).

[66] A. Ghoshal, S. Das, A. K. Pal, A. Sen(De), and U. Sen, Phys. Rev. A **104**, 042208 (2021).

[67] F. Barra, Scientific Reports **5**, 14873 (2015).

[68] P. Strasberg, G. Schaller, T. Brandes, and M. Esposito, Phys. Rev. X **7**, 021003 (2017).

[69] G. D. Chiara and A. Sanpera, Reports on Progress in Physics **81**, 074002 (2018).

[70] M. H. Mohammady, H. Choi, M. E. Trusheim, A. Bayat, D. Englund, and Y. Omar, Phys. Rev. A **97**, 042124 (2018).

[71] G. Thomas and R. S. Johal, Phys. Rev. E **83**, 031135 (2011).

[72] D. Türkpençe, F. Altintas, M. Paternostro, and O. E. Müstecaplioglu, EPL **117**, 50002 (2017).

[73] J. Lekscha, H. Wilming, J. Eisert, and R. Gallego, Phys. Rev. E **97**, 022142 (2018).

[74] M. Kloc, P. Cejnar, and G. Schaller, Phys. Rev. E **100**, 042126 (2019).

[75] Y. Hong, Y. Xiao, J. He, and J. Wang, Phys. Rev. E **102**, 022143 (2020).

[76] R. BS, V. Mukherjee, U. Divakaran, and A. del Campo, Phys. Rev. Research **2**, 043247 (2020).